Physica Medica 64 (2019) 222–229

Contents lists available at ScienceDirect

Physica Medica

journal homepage: www.elsevier.com/locate/ejmp

Original paper

Development of an IAEA phase-space dataset for the Leksell Gamma Knife® Perfexion™ using multi-threaded Geant4 simulations

Tae Hoon Kim[a], Thomas Schaarschmidt[a], Hye Jeong Yang[b], Yong Kyun Kim[a], Kook Jin Chun[c], Yona Choi[c], Hyun-Tai Chung[d,*]

[a] Department of Nuclear Engineering, Hanyang University, Seoul, Republic of Korea
[b] Department of Biomedical Engineering, College of Medicine, Catholic University of Korea, Seoul, Republic of Korea
[c] Department of Accelerator Science, Korea University Sejong Campus, Sejong, Republic of Korea
[d] Department of Neurosurgery, Seoul National University College of Medicine, Seoul, Republic of Korea

ARTICLE INFO

Keywords:
IAEA phase-space
Leksell Gamma Knife® Perfexion™
Geant4
Absorbed dose calculation

ABSTRACT

This study was conducted to develop a phase-space dataset in the International Atomic Energy Agency (IAEA) format for Monte Carlo (MC) simulations of the Leksell Gamma Knife® (LGK, Elekta Instrument AB, Stockholm, Sweden) Perfexion™ (PFX). An open-source MC code, namely, the Geant4 toolkit with a recently updated multi-threaded mode, was used to maximize the efficiency of the developed IAEA phase-space dataset. The absorbed dose profiles for single shots of the LGK PFX were calculated using the developed dataset and compared with those from radiochromic film measurements and Leksell GammaPlan® version 11.0.3 (LGP, Elekta Instruments) for verification. The mean relative absorbed dose differences in all single shots were less than 3.6% compared with the films and less than 4.0% compared with LGP. The collimator output factors were also calculated for all single shots and compared with the LGP results. The simulated collimator output factor was 0.816 ± 0.003 for a 4-mm shot and 0.903 ± 0.001 for an 8-mm shot in a spherical water phantom. The efficiency of the developed dataset was evaluated by comparing the times required for various simulations. Simulations with the phase-space dataset ran 25, 8.2 and 3.2 times faster than simulations without the phase-space dataset for 4-, 8-, and 16-mm shots, respectively. Using the dataset developed in this study, MC simulations of the LGK PFX can be performed more efficiently for various purposes, such as treatment plan verification and beam quality factor calculations.

1. Introduction

The Leksell Gamma Knife® (LGK, Elekta Instrument AB, Stockholm, Sweden) is a non-invasive stereotactic radiosurgery instrument that is used to treat tumours and functional disorders in the brain using gamma radiation from cobalt-60. The LGK model Perfexion™ (PFX), the successor to the model 4C, is used to treat patients in many hospitals. The PFX has capabilities exceeding those of the previous model 4C in terms of treatment efficiency, conformity, and radiation protection [1]. The PFX, unlike the model 4C with its 201 cobalt-60 sources, has 192 cobalt-60 sources arranged in 8 sectors. Each sector contains 24 sources and can move independently among five different positions; three of these positions are defined in reference to the collimator sizes of 4, 8, and 16 mm; the remaining two are a blocked position and a home position. By adjusting the sector configurations, a single isocentre of the PFX can be transformed into various shapes for absorbed dose distribution, rendering it significantly more efficient in treatment [1–3].

Leksell GammaPlan® version 11.0.3 (LGP, Elekta Instruments AB, Stockholm, Sweden), which is used to design treatment plans for an LGK unit, calculates the absorbed dose in a patient using the tissue-maximum ratio (TMR) 10 algorithm [4]. Because TMR 10 assumes that all material in the patient is water, there is an intrinsic error caused by the real inhomogeneity, the effects of which have been calculated in several studies using various Monte Carlo (MC) simulations [5–14]. Additionally, MC simulations have been increasingly used in assessing small-field and conformal radiation beams [15,16] because they are the most consistent tool for assessing dosimetric quantities [17]. However, a long computation time is required to perform MC simulations to calculate absorbed doses, especially for simulations of small-field beams such as in the LGK.

The Geant4 simulation toolkit, written in the object-oriented

* Corresponding author at: Department of Neurosurgery, Seoul National University College of Medicine, 101 Daehak-ro Jongno-gu, Seoul 03080, Republic of Korea.
E-mail address: htchung@snu.ac.kr (H.-T. Chung).

https://doi.org/10.1016/j.ejmp.2019.07.002
Received 19 April 2019; Received in revised form 7 June 2019; Accepted 1 July 2019
Available online 26 July 2019

language C++, simulates the tracks of particles through a particular geometry [18,19]. It is commonly used in high-energy physics and in medical applications. The Geant4 version 10 series was developed for enabling multi-threaded applications that share a substantial portion of data between threads to reduce memory usage. In the multi-threaded mode, each thread implements part of the event, enabling the simulation of one or multiple events through parallel processing [20]. Additionally, the phase-space method of reducing repetitive simulation steps when creating collimated beams can be employed to increase time efficiency for medical applications [21].

The International Atomic Energy Agency (IAEA) has designed projects for providing a public phase-space database for MC simulations of clinical photon beams [22]. Because the IAEA phase-space database is committed to the provision of input data for subroutines that use IAEA-format files, it is compatible with many commonly available simulation packages (e.g., Geant4, MCNP, and EGS) [22]. Several studies have used datasets that are freely available from the IAEA phase-space database for various clinical linear accelerators, which show good agreement with dosimetry references [23,24]. However, there is no dataset in the IAEA phase-space database associated with the LGK unit. Nevertheless, the ability to use the IAEA phase-space database to simulate LGK units, in addition to clinical linear accelerators, without details of the machine parameters would be beneficial to users.

In this study, we modelled all 15 different collimator types of the PFX using the Geant4 toolkit and obtained absorbed dose profiles and collimator output factors. The simulation results were compared with the reference data provided by the vendor. Then, we developed files containing phase-space data for all 15 collimators of the PFX using the IAEA phase-space interface, which was developed to work with the IAEA phase-space database and is capable of reading and writing in Geant4 [25,26]. The simulation results obtained using the developed phase-space data were compared with the results of radiochromic film measurements and LGP for verification. The simulation times with and without the developed dataset were compared to assess its efficiency.

2. Materials and methods

2.1. Single-collimator simulations

Regarding the collimators of the LGK PFX, there are three sets of collimator channels of different sizes, namely, 4, 8, and 16 mm, converging at the isocentre. For each collimator size, there are 192 channels distributed in five rings. These 192 channels are divided into eight sectors arranged at 45-degree separation angles around the Z-axis (Fig. 1(a)). The collimator size that is currently in use can be changed by moving the source tray (Fig. 1(b)). In each sector, there are 24 channels arranged in five rings for each collimator size; thus, in total there are 15 collimator types in the LGK PFX. The source-to-focus distance and source angle are different from one ring to another. The corresponding rings in each sector possess cylindrical symmetry with respect to the isocentre and have the same machine-specific parameters as provided by the vendor. Therefore, we performed single-collimator-channel simulations separately for only 15 collimator types (Fig. 1(c)).

To compare the simulation results with the reference data provided by the vendor, the absorbed dose profiles and the output factor at the isocentre of an 80-mm spherical water phantom were obtained. The profiles were calculated along the X′- and Y′-axes perpendicular to the single collimator at the isocentre with the sensitive volume divided into a grid of cubical voxels, each with a length of 0.25 mm for the 4-mm single collimators and a length of 0.5 mm for both the 8-mm and 16-mm single collimators. The output factor for each single collimator was calculated as the ratio of the absorbed dose in a simulation using that collimator to the absorbed dose in a simulation using the 16-mm, ring 2 collimator. The shapes and sizes of the sensitive volumes used to calculate the output factors were determined to correspond to a cube of 0.51 mm^3 for the 4-mm single collimators, a cube of 4.10 mm^3 for the 8-mm single collimators, and a cube of 32.77 mm^3 for the 16-mm single collimators. These values were based on a previous study that investigated the suitable volume and size of the sensitive volume such that the statistical error is minimized while the uniformity of the absorbed dose distribution is maximized [11].

The Penelope low-energy electromagnetic physics model for electrons, positrons, and photons in Geant4 version 10.3 was used. As previously done by Pipek et al. [11], the production cut value for secondary particle generation was set to 0.03 mm in all collimators, which are composed of high-Z materials. By contrast, in the phantom and in air, the production cut value was 990 eV, which is the minimum energy limit given in the physics list. Additionally, we confined the solid angle of primary photon generation to 3 degrees around the Z′-axis. This confinement angle was determined based on the results of previous studies for both model C [6] and the PFX model [11,13], wherein the optimal bias angle was examined.

2.2. IAEA phase-space data and single-shot simulations

IAEA-format phase-space data files for the three collimator sizes and five ring types of the PFX were created using the G4IAEAphspWriter class. A total of 15 phase-space data files were created in sequence and written in binary format along with a separate header file in ASCII format. For each data file, 3.2×10^9 primary photons were generated, and information on particles passing through a phase-space plane 125 mm away from the isocentre of the corresponding single collimator was collected (Fig. 1(c)). In the phase-space data file, the particle type, energy (E), statistical weight (w), Cartesian position components (x, y, and z), and directional components of linear momentum (u, v, and w) were recorded.

Using these phase-space data files for the LGK PFX, we then performed single-shot simulations in which all of the sectors were set to a particular collimator size. The single-shot simulations proceeded in order from sector 1 to sector 8. For sector 1, the phase-space data file corresponding to ring 1 and a particular collimator size was loaded using the G4IAEAphspReader class and rotated to the machine-specific angle with respect to the isocentre using the SetGlobalPhspTranslation function of the G4VPrimaryGeneratorAction class. The rotation angle was set at the machine-specific angle using the SetRotationX and SetRotationZ functions. Using the SetRotationOrder function, a rotation was first performed on the X-axis and then on the Z-axis. After the simulation run for one ring was completed, the phase-space file was closed, and the simulation for the next ring was then performed accordingly.

To avoid any duplication of the phase-space data file for the collimator channels in the same ring in one sector, the ParallelRun function of G4IAEAphspReader was used to divide the phase-space file into several chunks. In the case of ring 1, there are six channels of a given size in one sector, so the data file was divided into six chunks using the ParallelRun function. Similarly, the ring 2 simulation was performed by dividing the corresponding phase-space data file into four chunks. In this way, a total of 24 simulations using five properly divided data files were performed per sector. The eight sectors in each single-shot simulation were covered simply by rotating the same sector in increments of 45 degrees with respect to the Z-axis. Because each phase-space data file was used repeatedly in the 8 sectors, it was recycled up to 8 times.

To successfully apply the developed phase-space dataset in multi-threaded mode, the user source code had to be written with care with regard to memory handling. The G4Controller class was used to load the dataset and allow all threads to access it. Then, each event was simulated independently, and this procedure was repeated on all threads. A summary diagram of the overall simulation process for a 4-mm single shot of the PFX using the developed IAEA phase-space dataset in multi-threaded mode is shown in Fig. 2.

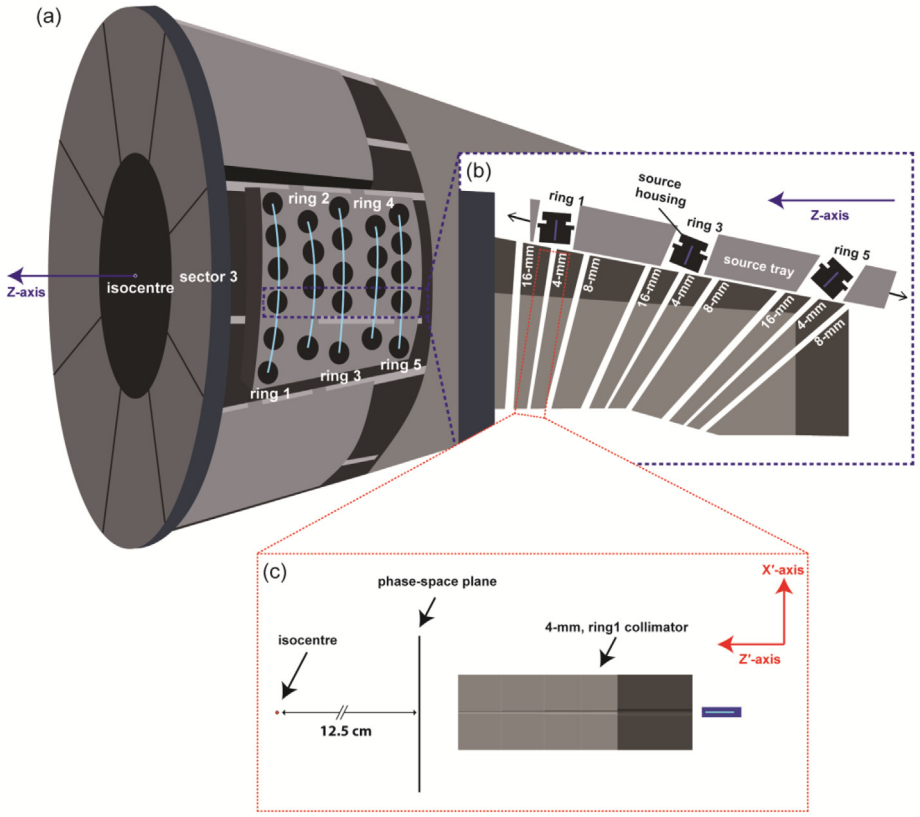

Fig. 1. (a) Overall diagram of the Leksell Gamma Knife® Perfexion™ collimation system. (b) Cross section of the collimator channels and source tray for rings 1, 3, and 5 of one sector in the 4-mm collimator position. (c) Cutaway view of the 4-mm, ring 1 single collimator modelled in Geant4.

2.3. Verification of the phase-space dataset

For the verification of single-shot simulations using the developed phase-space dataset, absorbed dose profiles for 4-, 8-, and 16-mm single shots of the PFX at the isocentre of a spherical phantom were obtained and compared with the results of film measurements and LGP. The collimator output factors for the 4-mm and 8-mm single shots were also calculated as the ratio of the corresponding absorbed dose in the sensitive volume to the absorbed dose for a 16-mm collimated beam at the isocentre of the spherical phantom. The dimensions of the sensitive volumes used to calculate the absorbed dose profile and output factor for each collimator size were the same as those outlined in Section 2.1. Simulations were performed for two different spherical phantom materials: water and Solid Water® (Gammex RMI, Middleton, WI, USA). The physical density and the elemental mass percent composition of these materials are shown in Table 1 [27].

The absorbed dose profiles of the LGK PFX were measured using Gafchromic® EBT3 films (International Specialty Products, NJ, USA) at Seoul National University Hospital. The films were cut into 60 × 60-mm^2 square shapes and inserted at the centre of a vendor-provided dosimetry phantom (Elekta AB, Stockholm, Sweden) made of Solid Water® (Fig. 3(a)). Before the absorbed dose profiles were obtained, the

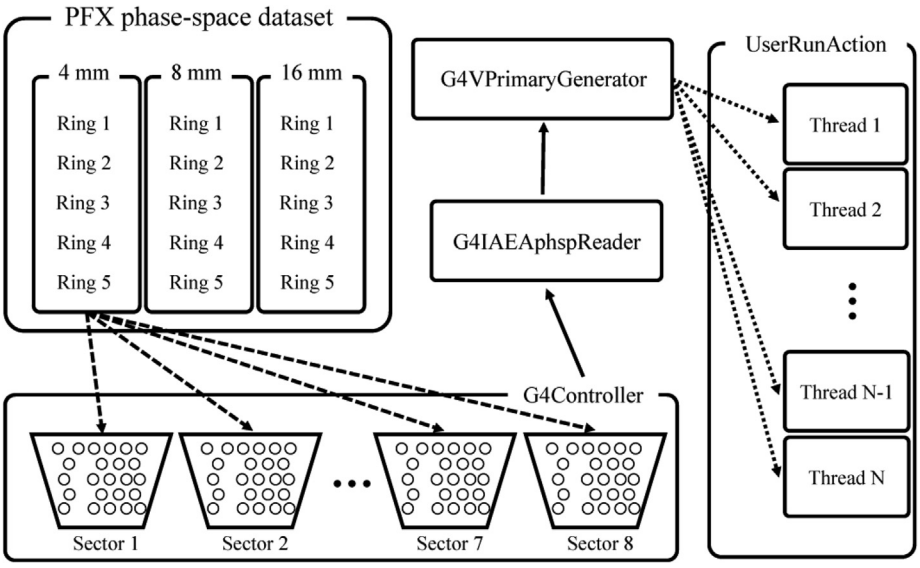

Fig. 2. A 4-mm single-shot simulation diagram using the Leksell Gamma Knife® Perfexion™ (PFX) phase-space dataset. The G4Controller reads the database in accordance with the user-specified configuration (dashed lines). The diagram shows the process by which the multi-threaded mode is implemented with N threads (dotted lines).

Table 1
The density and elemental mass percent composition of the phantom material used in the simulation.

Material	Density (g/cm^3)	Mass percent composition (%)					
		H	C	N	O	Cl	Ca
Water	1.000	11.1	–	–	88.9	–	–
Solid Water®	1.043	8.1	67.2	2.4	19.9	0.1	2.3

* Refer to the Gammex 457-CTG, by Gammex, Inc.

films were calibrated by irradiating them in 1-Gy increments from 0 to 10 Gy using 16-mm single shots. At 4 days after irradiation, the films were scanned to obtain images in 48-bit uncompressed TIF format using a flatbed scanner, an Epson Expression 10000 XL (Epson Seiko Corporation, Nagano, Japan). The scan resolution was 300 DPI, and one of the scanned images is shown in Fig. 3(b). Optical densities were calculated using the red channel values of the image files, and a calibration curve for converting optical densities into absorbed doses was obtained by fitting the calibration data using a third-order polynomial. During the irradiation and analysis of the films, their orientation was carefully maintained for consistency [28].

2.4. Efficiency of using the phase-space dataset

To evaluate the computational efficiency achieved when using the developed phase-space dataset, the total CPU times of single-shot simulations performed with and without the dataset were compared for various numbers of primary photons. We also compared the total CPU times with and without the phase-space dataset for each single-shot simulation. The simulations were performed in multi-threaded mode using a workstation with two Xeon® E5-2687 W v4 CPUs (3.00 GHz, 12 cores, 24 threads, Intel®, California, USA).

3. Results

3.1. Verification of the single-collimator simulations

The absorbed dose profiles obtained in the simulations of the 15 types of PFX single collimators were compared with the vendor-provided reference data. The profiles for ring 2 close to the isocentre are shown in Fig. 4 and were analysed for all collimator sizes. When we compared the absorbed doses at points that received at least 10% of the maximum dose, along the X′-axis, the mean relative absorbed dose differences were 2.7%, 2.6%, and 2.5% for the 4-, 8-, and 16-mm collimators, respectively. Along the Y′-axis, the mean relative absorbed dose differences were 3.1%, 3.1%, and 2.6% for the 4-, 8-, and 16-mm collimators, respectively. The collimator output factors were calculated for all collimator configurations and compared with the reference data, and the results are shown in Table 2. The differences in the collimator output factors were less than 0.9%.

3.2. Composition and verification of the phase-space dataset

The IAEA phase-space data files for all 15 collimator configurations were created by generating 3.2×10^9 primary photons for each setup. Information on all particles (mainly photons, electrons, and positrons) impinging on the phase-space plane was recorded. The total dataset size is 58.1 GB, while the size of each file depends on the collimator size and ring number. The number and energy information of particles in each data file is shown in Table 3.

In the single-shot simulations, 5×10^8 particles (mainly photons) extracted from the phase-space dataset for all rings were simulated for each of the 192 channels, such that 9.6×10^{10} photons were generated. The absorbed dose profiles for single shots with the 4-, 8-, and 16-mm collimators were obtained at the centre of a spherical phantom with a radius of 80 mm, as shown in Fig. 5. For the phantom composed of water, the mean relative differences along the X-axis between the results obtained with the EBT3 film and the simulated absorbed dose profiles were 2.8%, 2.1%, and 1.2% for the 4-, 8-, and 16-mm collimators, respectively. The associated relative absorbed dose differences along the Z-axis were 2.6%, 3.6%, and 2.5%. For the Solid Water® phantom, the differences along the X-axis with respect to the absorbed dose profiles obtained with the EBT3 film were 2.9%, 2.0%, and 1.2% for the 4-, 8-, and 16-mm collimators, respectively. The associated relative absorbed dose differences along the Z-axis were 2.6%, 3.3%, and 2.6%. For the phantom composed of water, the mean relative differences along the X-axis between the LGP results and the simulated absorbed dose profiles were 1.2%, 2.1%, and 1.1% for the 4-, 8-, and 16-mm collimators, respectively. The associated relative absorbed dose differences along the Z-axis were 2.0%, 3.9%, and 4.0%, respectively. For the Solid Water® phantom, the differences along the X-axis with respect to the absorbed dose profiles obtained with LGP were 1.4%, 2.1%, and 1.1% for the 4-, 8-, and 16-mm collimators, respectively. The associated relative absorbed dose differences along the Z-axis were 2.2%, 3.8%, and 4.0%.

The collimator output factors obtained for the water phantom and the Solid Water® phantom are presented in Table 4, together with the LGP values and EBT3 film measurements. The output factor of the EBT3 film was calculated based on the area of the volume used in the

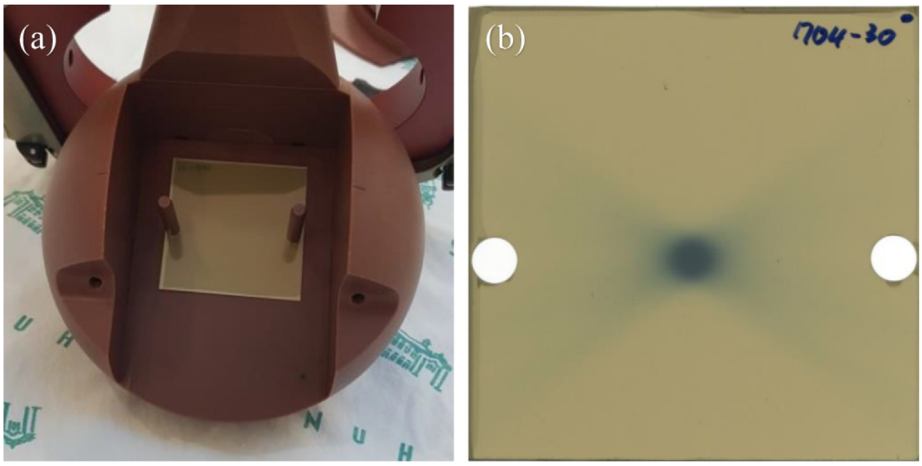

Fig. 3. (a) Spherical dosimetry phantom fabricated of Solid Water® (Gammex RMI, Middleton, WI, USA) with an EBT3 (International Specialty Products, NJ, USA) film inserted in the measurement setup. (b) Scanned image of an EBT3 film irradiated with a 4-mm single shot from the Leksell Gamma Knife® Perfexion™.

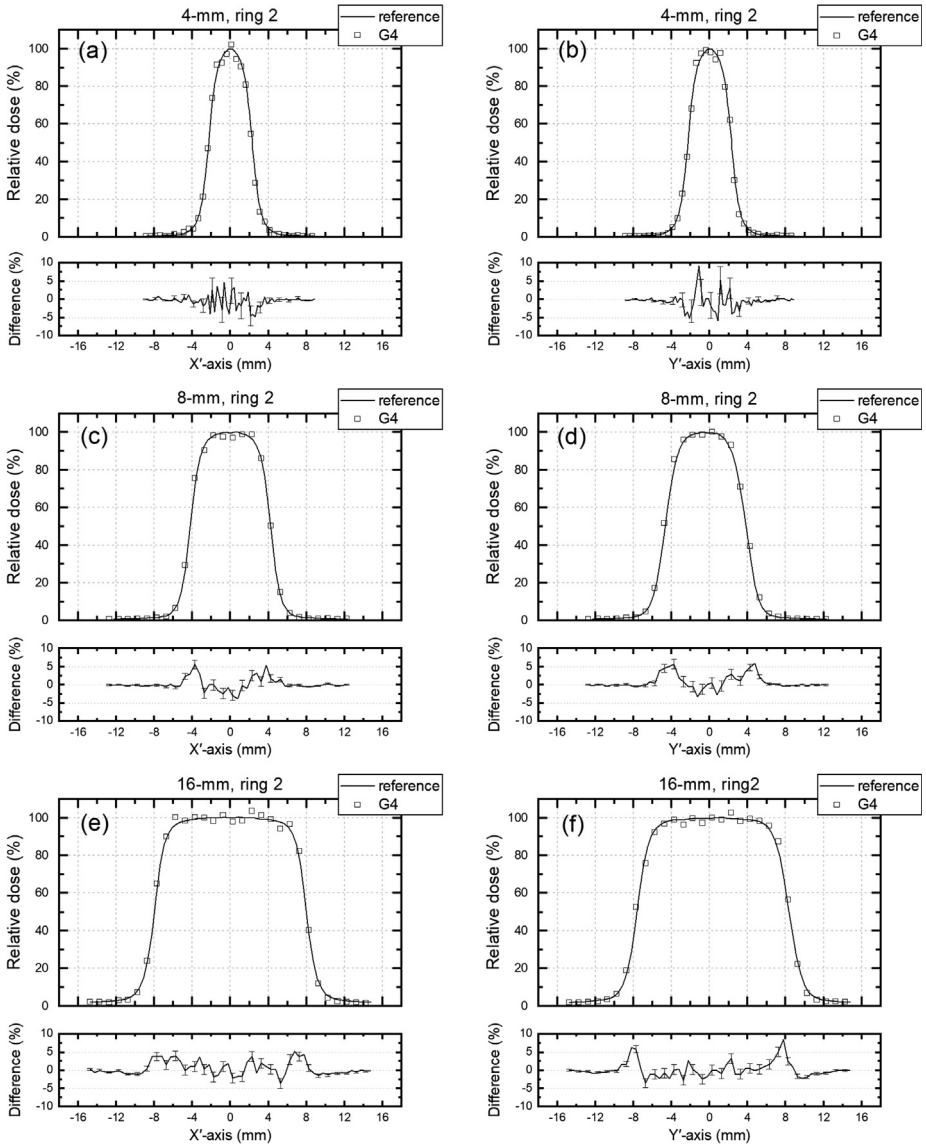

Fig. 4. One-dimensional absorbed dose profiles for single collimators in ring 2 as obtained in this simulation (squares) and as indicated by the reference data (solid lines). The X′-axis and Y′-axis profiles for a 4-mm collimator (a and b), an 8-mm collimator (c and d) and a 16-mm collimator (e and f) are shown. The relative absorbed dose differences and uncertainties are also presented under the profiles.

Table 2
Collimator output factors from this study compared with the reference data.

Collimator size	Ring	Reference	This study	Difference (%)
4 mm	1	0.812	0.809 ± 0.017	−0.33
	2	0.823	0.816 ± 0.017	−0.89
	3	0.795	0.802 ± 0.017	0.86
	4	0.726	0.728 ± 0.016	0.22
	5	0.664	0.664 ± 0.015	−0.07
8 mm	1	0.934	0.930 ± 0.008	−0.45
	2	0.919	0.920 ± 0.009	0.15
	3	0.874	0.874 ± 0.008	−0.02
	4	0.782	0.777 ± 0.008	−0.69
	5	0.708	0.706 ± 0.007	−0.27
16 mm	1	0.961	0.960 ± 0.005	−0.10
	2	1	1	–
	3	0.981	0.979 ± 0.005	−0.20
	4	0.914	0.910 ± 0.005	−0.44
	5	0.847	0.843 ± 0.005	−0.48

simulation. The differences between LGP and Geant4 simulations were less than 0.3% in both simulations. The output factors calculated for the Solid Water® phantom were also close to the output factors obtained for the water phantom.

3.3. Efficiency of using the phase-space dataset

We performed 4-mm single-shot simulations with numbers of generated primary photons ranging from 1.9×10^7 to 9.6×10^{10} with and without the phase-space dataset, and the results of three executions are shown in Fig. 6(a). When the phase-space dataset was not used, the simulation time increased linearly with the number of primary particles. When the phase-space dataset was used, a fixed amount of time was spent for simulations with fewer primary particles, and the time began to increase once the number of primary particles increased past a certain threshold. Fig. 6(b) shows the execution times for simulations of single shots with the three collimator sizes and 9.6×10^{10} primary photons with and without the phase-space dataset. The increase in efficiency achieved when using the dataset was the highest for the 4-mm simulation, which ran 25 times faster, because most of the primary

Table 3
Number (N) of particles and minimum (E_{min}), maximum (E_{max}) and mean ($\overline{E}$) energy of particles stored in the phase-space dataset for all collimators and rings of the Leksell Gamma Knife® Perfexion™. The number of particles initially generated in all 15 collimators was 3.2×10^9.

Collimator size	Ring	Photons				Electrons			
		N ($\times 10^8$)	E_{min} (KeV)	E_{max} (MeV)	$\overline{E}$ (MeV)	N ($\times 10^5$)	E_{min} (KeV)	E_{max} (MeV)	$\overline{E}$ (MeV)
4 mm	1	0.24	2.93	1.33	1.23	0.45	0.51	1.32	0.62
	2	0.25	1.79	1.33	1.23	0.45	0.15	1.32	0.62
	3	0.26	2.03	1.33	1.24	0.43	0.01	1.31	0.63
	4	0.23	2.93	1.33	1.24	0.36	0.22	1.31	0.63
	5	0.21	2.93	1.33	1.24	0.30	0.00	1.32	0.64
8 mm	1	0.88	1.23	1.33	1.24	1.85	0.13	1.33	0.62
	2	0.89	1.51	1.33	1.24	1.68	0.00	1.32	0.63
	3	0.86	1.13	1.33	1.25	1.51	0.00	1.31	0.64
	4	0.72	1.11	1.33	1.25	1.19	0.14	1.33	0.64
	5	0.67	1.80	1.33	1.25	1.04	0.03	1.31	0.65
16 mm	1	2.98	1.19	1.33	1.25	6.61	0.00	1.33	0.62
	2	3.11	1.00	1.33	1.25	6.57	0.00	1.32	0.62
	3	3.13	1.12	1.33	1.24	6.62	0.00	1.33	0.62
	4	2.90	1.02	1.33	1.25	5.61	0.00	1.33	0.63
	5	2.66	1.30	1.33	1.25	4.75	0.00	1.33	0.63

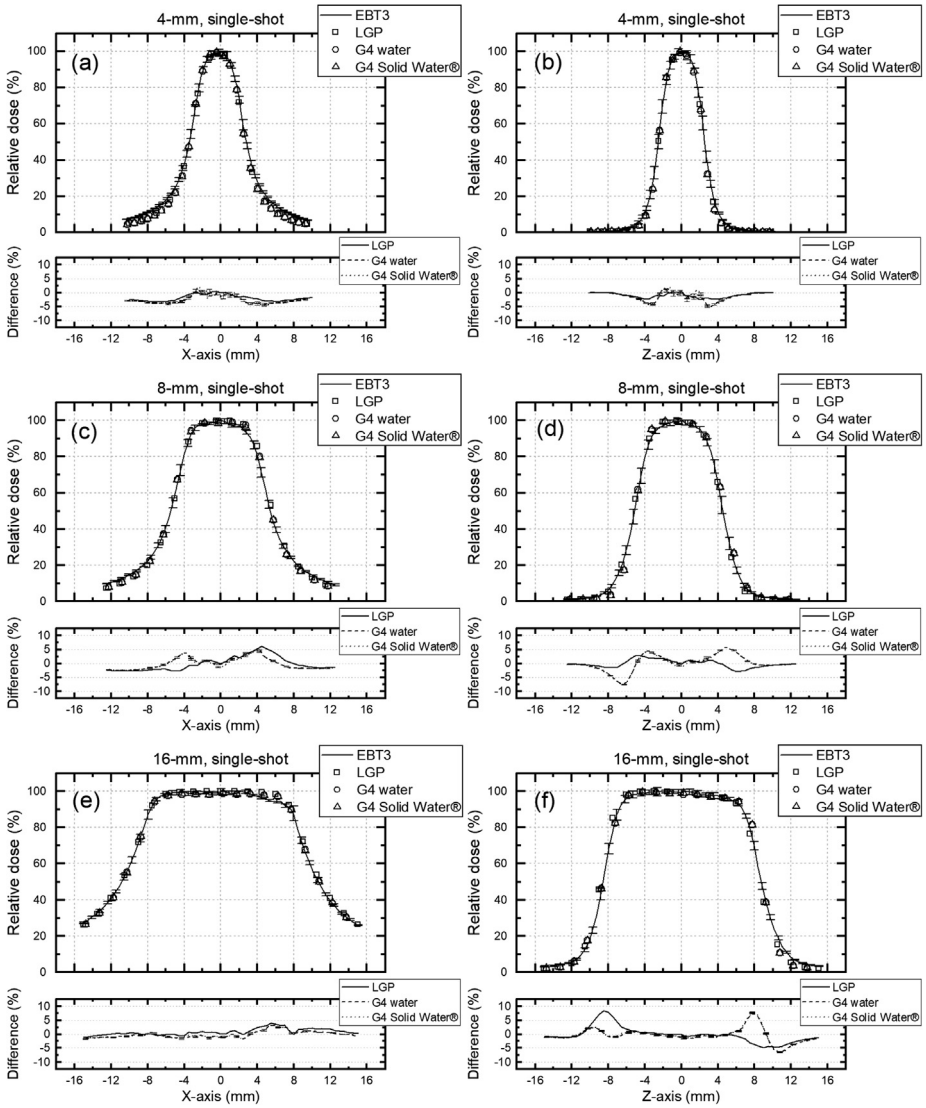

Fig. 5. One-dimensional absorbed dose profiles as obtained from Gafchromic™ EBT3 film, Leksell GammaPlan® (LGP), and Geant4 simulations (G4) for two different spherical phantom materials. The X-axis and Z-axis profiles for a 4-mm collimator (a and b), an 8-mm collimator (c and d), and a 16-mm collimator (e and f) are shown. The relative absorbed dose differences and uncertainties are shown beneath the profiles. The EBT3 film uncertainties are shown overlaid on the profiles, and the simulation uncertainties are shown beneath the profiles.

Table 4
Collimator output factors (OFs) and differences between the results of the current study and Leksell GammaPlan® version 11.0.3 (LGP).

Collimator size	EBT3	LGP	Geant4 water		Geant4 Solid Water®	
			OF	Difference	OF	Difference
4 mm	0.801 ± 0.032	0.814	0.816 ± 0.003	0.23%	0.812 ± 0.003	−0.24%
8 mm	0.890 ± 0.037	0.900	0.903 ± 0.001	0.30%	0.901 ± 0.001	0.07%

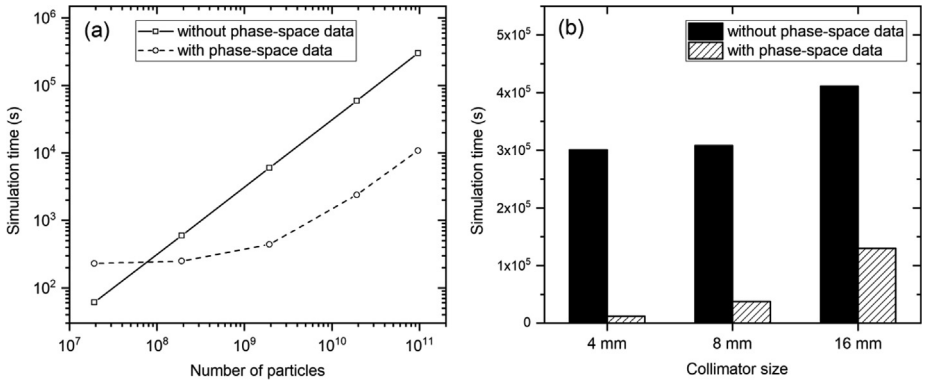

Fig. 6. (a) Execution times required for simulations of 4-mm single shots with various numbers of generated primary photons. (b) Execution times for simulations with 9.6×10^{10} primary photons with and without the phase-space dataset.

photons do not traverse the collimator and are wasted in this case. The simulations with the phase-space dataset ran 8.2 and 3.2 times faster than the simulations without the phase-space dataset for the 8- and 16-mm shots, respectively.

4. Discussion

The present study was performed to build an IAEA-format phase-space dataset for the simulation of an LGK PFX. The results of Geant4 simulations of single collimators showed good agreement with the vendor-provided reference data; therefore, such a phase-space dataset could be successfully generated using the model. The single-collimator profiles were in good agreement with the reference data for both the plateau region and the penumbra region (Fig. 4), and the errors on the output factors obtained from our simulations for single collimators (less than 0.9%) were similar to the errors published in other studies (Table 2). Pipek et al. reported output factor errors of less than 1.0% for all collimators and rings [11]. A study by Yuan et al. showed that the errors on the output factors were less than 0.7% for all collimators and rings [14].

The simulation results obtained using the IAEA phase-space dataset developed with the single-collimator code also showed good agreement with film measurements and LGP profiles. Regarding the one-dimensional absorbed dose profiles for a single shot from a PFX, Yuan et al. reported a < 2% absorbed dose difference in the plateau region and a < 5% difference in the penumbra region. These results are similar to the results of this study, which found differences of 1% and 9%, respectively. Pipek et al. reported that the error on the output factor was 0.9% for a 4-mm single shot and 0.4% for an 8-mm single shot [11]. Compared with the results of studies using sensitive detectors similar to those in the present study, our collimator output factors showed smaller differences, i.e., less than 0.3% with respect to the LGP data (Table 4). Interestingly, the collimator output factors obtained for the Solid Water® phantom showed no difference from those obtained for the water phantom. The output factors measured with EBT3 films showed similar results to the study of Zeverino et al. (0.797 ± 0.032 for 4-mm, 0.887 ± 0.035 for 8-mm) [29], and our simulation results were within the error range.

The most valuable benefit of using the developed phase-space dataset is the reduction in the execution time for simulations. With our database, the simulation time could be reduced by a factor of 25 in the case of a 4-mm single-shot simulation. Because multiple shots with different collimator sizes are used in real patient treatments, the effective reduction ratio may be smaller, for example, closer to three in a case in which all shots use the 16-mm collimator size. When the number of primary photons was small, for example, less than 7.7×10^7 for a 4-mm shot simulation, simulations with the developed dataset took longer because a certain amount of time is necessary to sequentially open and close the data files 192 times for a single-shot simulation. However, in most cases, simulations with the developed phase-space dataset are both efficient and accurate because a sufficiently large number of photons is needed to reduce uncertainty.

5. Conclusion

We developed a dataset for inclusion in the IAEA phase-space database that can be used to simulate the LGK PFX and verified its accuracy. Simulations of single shots using the developed phase-space dataset showed good agreement with LGP results and film measurements. When the phase-space dataset was used for PFX single-shot simulations, the simulation times were reduced by a factor of 3–25 for simulations with 9.6×10^{10} primary particles. We allowed the phase-space data to be accessed from all threads in simulations in multi-threaded mode. The IAEA-format phase-space dataset for the LGK PFX developed in this study could reduce repetitive work in simulations of more complex scenarios and could be useful to many users who do not need to know the details of the machine, which are not always provided by the vendor.

Acknowledgements

This study was supported by the Ministry of Trade, Industry and Energy (grant number 10069168) and the Ministry of Science and ICT (grant number NRF-2016M2A2A6A03946564).

References

[1] Lindquist C, Paddick I. The Leksell Gamma Knife Perfexion and comparisons with its

predecessors. Operative Neurosurgery 2007;61. ONS-130-ONS-41.
[2] Novotny J, Bhatnagar JP, Niranjan A, Quader MA, Huq MS, Bednarz G, et al. Dosimetric comparison of the Leksell Gamma Knife perfexion and 4C. J Neurosurg 2008;109:8–14.
[3] Niranjan A, Novotny Jr J, Bhatnagar J, Flickinger JC, Kondziolka D, Lunsford LD. Efficiency and dose planning comparisons between the Perfexion and 4C Leksell Gamma Knife units. Stereotact Funct Neurosurg 2009;87:191–8.
[4] Elekta Instrument A. A new TMR dose algorithm in Leksell GammaPlan. Technical Report 2011.
[5] Cheung JY, Yu K, Yu C, Ho RT. Monte Carlo calculation of single-beam dose profiles used in a gamma knife treatment planning system. Med Phys 1998;25:1673–5.
[6] Al-Dweri FM, Lallena AM, Vilches M. A simplified model of the source channel of the Leksell GammaKnife® tested with PENELOPE. Phys Med Biol 2004;49:2687.
[7] Romano F, Sabini M, Cuttone G, Russo G, Mongelli V, Foroni R. Geant4-based Monte Carlo Simulation of the Leksell Gamma Knife®. Nuclear Science Symposium Conference Record, 2007 NSS'07 IEEE. IEEE; 2007. p. 2581–6.
[8] Trnka J, Novotny Jr J, Kluson J. MCNP-based computational model for the Leksell Gamma Knife. Med Phys 2007;34:63–75.
[9] Ma L, Kjäll P, Novotny Jr J, Nordström H, Johansson J, Verhey L. A simple and effective method for validation and measurement of collimator output factors for Leksell Gamma knife® Perfexion™. Phys Med Biol 2009;54:3897.
[10] Battistoni G, Cappucci F, Bertolino N, Brambilla MG, Mainardi HS, Torresin A. FLUKA Monte Carlo simulation for the Leksell Gamma Knife Perfexion radiosurgery system: homogeneous media. Physica Med 2013;29:656–61.
[11] Pipek J, Novotný J, Novotný Jr J, Kozubíková P. A modular Geant4 model of Leksell Gamma knife perfexion™. Phys Med Biol 2014;59:7609.
[12] Benmakhlouf H, Johansson J, Paddick I, Andreo P. Monte Carlo calculated and experimentally determined output correction factors for small field detectors in Leksell Gamma Knife Perfexion beams. Phys Med Biol 2015;60:3959.
[13] Pappas E, Moutsatsos A, Pantelis E, Zoros E, Georgiou E, Torrens M, et al. On the development of a comprehensive MC simulation model for the Gamma Knife Perfexion radiosurgery unit. Phys Med Biol 2016;61:1182.
[14] Yuan J, Lo SS, Zheng Y, Sohn JW, Sloan AE, Ellis R, et al. Development of a Monte Carlo model for treatment planning dose verification of the Leksell Gamma Knife Perfexion radiosurgery system. J Appl Clin Med Phys 2016;17:190–201.
[15] Das IJ, Ding GX, Ahnesjö A. Small fields: nonequilibrium radiation dosimetry. Med Phys 2008;35:206–15.
[16] Cranmer-Sargison G, Weston S, Evans J, Sidhu N, Thwaites D. Implementing a newly proposed Monte Carlo based small field dosimetry formalism for a comprehensive set of diode detectors. Med Phys 2011;38:6592–602.
[17] Andreo P. Monte Carlo techniques in medical radiation physics. Phys Med Biol 1991;36:861.
[18] Agostinelli S, Allison J, Ka Amako, Apostolakis J, Araujo H, Arce P, et al. GEANT4—a simulation toolkit. Nuclear instruments and methods in physics research section A: accelerators, spectrometers, detectors and associated. Equipment 2003;506:250–303.
[19] Allison J, Amako K, Apostolakis J, Araujo H, Dubois PA, Asai M, et al. Geant4 developments and applications. IEEE Trans Nucl Sci 2006;53:270–8.
[20] Allison J, Amako K, Apostolakis J, Arce P, Asai M, Aso T, et al. Recent developments in Geant4. Nucl Instrum Methods Phys Res, Sect A 2016;835:186–225.
[21] Libby B, Siebers J, Mohan R. Validation of Monte Carlo generated phase-space descriptions of medical linear accelerators. Med Phys 1999;26:1476–83.
[22] Capote R, Jeraj R, Ma C, Rogers D, Sánchez-Doblado F, Sempau J, et al. Phase-space database for external beam radiotherapy. Summary report of a consultants' meeting. International Atomic Energy Agency; 2006.
[23] Rucci A, Carletti C, Cravero W, Strbac B. Use of IAEA's phase-space files for the implementation of a clinical accelerator virtual source model. Physica Med 2014;30:242–8.
[24] Aboulbanine Z, El Khayati N. Validation of a virtual source model of medical linac for Monte Carlo dose calculation using multi-threaded Geant4. Phys Med Biol 2018;63:085008.
[25] Cortés-Giraldo MA, Quesada JM, Gallardo MI, Capote R. Geant4 interface to work with IAEA phase-space files. 2009.
[26] Cortés-Giraldo MA, Quesada JM, Gallardo MI, Capote R. An implementation to read and write IAEA phase-space files in GEANT4-based simulations. Int J Radiat Biol 2012;88:200–8.
[27] Water CTGS. Gammex 457-CTG, by Gammex, Inc.
[28] Niroomand-Rad A, Blackwell CR, Coursey BM, Gall KP, Galvin JM, McLaughlin WL, et al. Radiochromic film dosimetry: recommendations of AAPM radiation therapy committee task group 55. Med Phys 1998;25:2093–115.
[29] Zeverino M, Jaccard M, Patin D, Ryckx N, Marguet M, Tuleasca C, et al. Commissioning of the Leksell Gamma Knife® Icon™. Med Phys 2017;44:355–63.